Ring Device to Induce Hemostasis

A Technical Report submitted to the Department of Biomedical Engineering

Presented to the Faculty of the School of Engineering and Applied Science

University of Virginia • Charlottesville, Virginia

In Partial Fulfillment of the Requirements for the Degree

Bachelor of Science, School of Engineering

Piper O'Donnell

Spring, 2022

Technical Project Team Members

Roan Back

On my honor as a University Student, I have neither given nor received unauthorized aid on this assignment as defined by the Honor Guidelines for Thesis-Related Assignments

Dr. William Guilford, Department of Biomedical Engineering

Ring Device to Induce Hemostasis

Roan Back and Piper O'Donnell

Number of words: 2,809
Number of figures and tables: 8
Number of supplements: 3
Number of references: 25

Advisor:
Dr. William Guilford, Department of Biomedical Engineering at the University of Virginia

Advisor Signature:

Ring Device to Induce Hemostasis

Roan Back and Piper O'Donnell

Abstract

Skin cancer is the most common type of cancer in the United States. Mohs Micrographic Surgery (MMS) is the gold standard in treating the two most common skin cancers. In MMS however, nearly 45% of complications are due to excessive bleeding. Therefore, we strove to design a ring device to be used during MMS to achieve intraoperative hemostasis that could also be used in tandem with an electrosurgical pen as well as withstand the autoclave. Many designs were made in Autodesk Fusion 360 then 3D printed in polylactic acid. Two designs were chosen to be 3D printed in stainless steel after qualitative and quantitative analysis. These steel prototypes were polished and tested for efficacy using physical models. The physical models consisted of silicone gel in a petri dish with a canal to act as a blood vessel and a portion of silicone removed from the center to simulate the cancerous tissue removed. As liquid perfused through the vessel, the prototype was applied to the circumference of the "wound" and flow was stopped. The average force needed to close the vessel compared favorably with the amount of force predicted by a clinician. Finally, the rings of the devices were coated in an insulation material to enable use with an electrosurgical pen. A virtual model of the cheek and forehead were developed in Fusion. A canal was cut through the models to simulate an open vessel. A steel ring was placed atop of the skin layer with an applied load. It was expected that the vessel would close under pressure, but due to limitations in the precision of the computational mesh, vessel closure was not observed (even under 100N). Given the devices induced hemostasis at the expected force, the next step would be to test on patients and optimize the manufacturing practices.

Keywords: Mohs Micrographic Surgery, excessive bleeding, hemostasis, stainless-steel device

Introduction

Mohs Micrographic Surgery (MMS) is a surgical procedure that is used by clinicians to remove skin tissue that contains cancerous cells while leaving as much healthy tissue as possible. Frequently performed by certified dermatologists, MMS is known as the gold standard to treat various forms of skin cancer including basal cell carcinomas and squamous cell carcinomas[1]. With skin cancer being the most common form of cancer in the United States, it is estimated that 1 in 5 Americans will develop skin cancer within their lifetime[2]. An integral part of the procedure is creating hemostasis; a difficulty in achieving hemostasis may induce patient and physician anxiety, frustration, and a compromised surgical experience. Such a complication may also cause increased scarring or postoperative bleeding[3]. However, difficulty in inducing hemostasis is not a rare occurrence in MMS. Nearly 40% of complications that occur during MMS are a result of excessive bleeding[4].

The creation of a device that would control the state of hemostasis in MMS would better allow clinicians to better avoid excessive bleeding events. Hemostasis can be achieved through the application of manual pressure where the pressure cinches the blood vessels closed. Once the vessels are closed, clinicians can then use an electrosurgical device to cauterize the vessels closed. Without the initial inhibition of blood flow with the created device however, electrosurgical devices are much less effective at cauterizing vessels.

Prior art shows that clinicians have sought out a device that was able to induce hemostasis for punch biopsy procedures. We are aware of two separate devices, published by Dr. Edmund Walsh in 1950[5] (Supplementary Figure 1a) and Dr. Raymond Osbourn in 1954[6] (Supplementary Figure 1b) respectively, that were rings designed for the purpose of creating hemostasis. Dr. Walsh's design was intended to better the process of taking punch biopsies. The device was able to control or limit the movement of the skin surrounding the intended biopsy

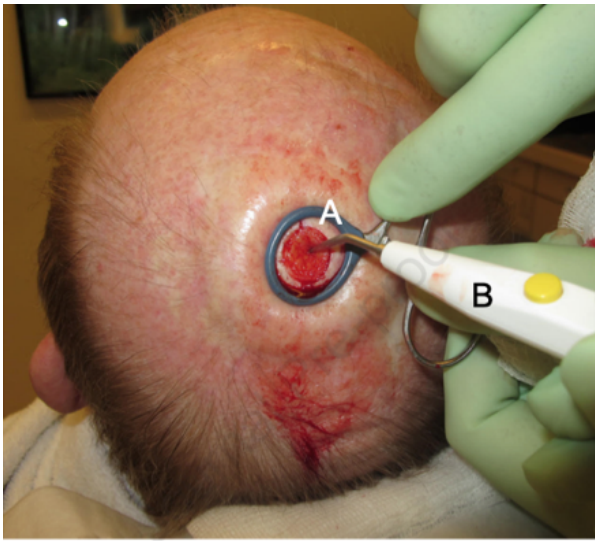

Figure 1. Use of a Suboptimal Device in Achieving Hemostasis. A) Ring and Handle and B) Electrosurgical Pen. The electrosurgical pen uses electricity to quickly cauterize the blood vessel to help stop the bleeding. Photo courtesy of Lee and Russell, 2021.

point, and the pressure application would force the intended biopsy point within the ring to protrude above the surface of the surrounding skin or tissue. However, since the device was not intended for use outside of punch biopsies, the dimensions of the ring were 10 or 12 mm (as there were two models), which is seemingly small for use in most other applications. The device was also not designed to be used in conjunction with any electrosurgical tool. Dr. Osbourn built upon the vision of Dr. Walsh, however he was critical of the design. Dr. Osbourn was fearful that the metallic material would be a potential danger to both a patient and a clinician if the device was used in conjunction with electrodesiccation. Instead, Dr. Osbourn made his version of the device using a plastic material. Also, in his design, Osbourn included two rings on opposite sides of a single arched handle; the rings were 15mm and 10mm in diameter respectively. The rings on the device have a height of 6mm and a flat top and bottom, where it may come in contact with skin. After the creation of this device, Osbourn was advised that it was not marketable and to forgo any attempt to mass produce it.

In 2022 there is still a clinical desire for such a device. Dr. Mark Russell is a clinician that performs MMS and he uses the circular portion of a hemostat handle that is coated in an insulation material to induce hemostasis while performing the procedure as seen in Figure 1[3]. To do this, Russell holds the clamp portion of the hemostat in his hand. Clearly, as the hemostat is not built for this use the device is not optimized for comfort or stability when used in this manner. However, a benefit of the device that Russell uses is that it can be used in conjunction with electrosurgical devices due to the insulation coating. It can also be autoclaved for continued use.

Our device allows a clinician to induce hemostasis through manual compression with a single hand, leaving their secondary hand available for use of electrosurgical instruments. The points of the device that may come in contact with electrosurgical tools are to be coated in an insulation material so that the device may be used in conjunction with electrosurgical devices. The device is designed with a base material of stainless steel, meaning the device can be autoclaved for continued use. The ring size on our device will also be enlarged to be optimal for use in procedures such as MMS or melanoma excision. The handle of the device is designed to allow for clinician comfort and stability throughout the procedure and during prolonged periods of pressure application. In addition, the rings on the device are rounded to allow for the clinician to better manipulate the device as it allows them to "roll" the device to find points of excessive bleeding. The clinician can identify sites of bleeding across a particular portion of the incision line while maintaining hemostasis at other portions of the incision. As the clinician is better able to identify individual vessels that are bleeding significantly, the ability of the clinician to inhibit an extreme bleeding event from occurring with the full removal of the device improves.

In collaboration with a UVA Dermatology clinician, optimal dimensions and design of a possible device were discussed. From these design considerations, various generations of designs were prototyped. After each generation of models, clinician feedback was collected to redesign the future generation of prototypes. Particular design considerations were taken into consideration due to clinical feedback. Clinicians found the length of the handle, the size of the rings, and the shape of the rings to be dimensions of importance. The length of the handle of the device needed to be able to comfortably fit the hand of a clinician. The rings needed to be of a proper size to surround the incision line made. The rings needed to be able to roll along the surface of the skin. These design constraints were used to design the mentioned multiple generations of designs.

To test the designs that were ultimately chosen to be prototyped, both physical and computational models were designed to test the functionality of the device. The device needs to be able to withstand particular levels of pressure applied by the clinician, while also causing no damage to the tissue to which it was applied. Methodology of designing the models will be discussed in a later section.

Results

The final models were chosen based on feedback from a Mohs surgeon and the results of the finite element analysis (Figure 2a). Model B has a straight handle length of 4cm and a total handle length of 13cm in the x direction. The height of the model is 2 cm. The inner ring diameters on both models are 2.5 cm and 3.5 cm with a ring thickness of 4 mm. Both models also have an attachment angle between the ring and the handle of 150 degrees. Model E has a handle length of 14 cm. Models B and E were printed in stainless steel using direct metal laser sintering (DMLS). Stainless steel was chosen because of its corrosion resistance and ease of sterilization. This process had to be conducted twice due to the issues with the supports needed to make the print. The stainless-steel prototypes were printed onto a steel plate (Figure 2b). A mallet and pliers were used to remove the prototypes from the plate before polishing. We used a file to remove imperfections and a buffer wheel with two separate grit levels for a finishing polish (Figure 3).

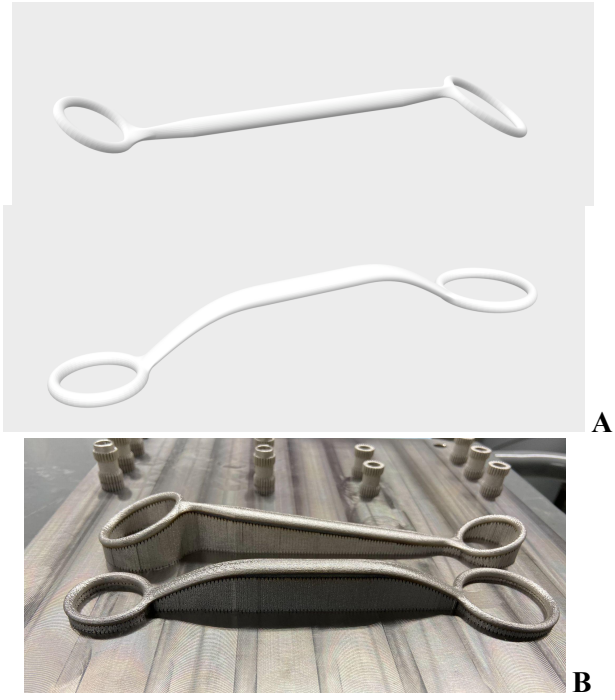

Figure 2. Final Chosen Designs. (a) Final Designs shown in CAD (b) Final designs shown printed in DMLS with supports.

Once the prototypes were polished, they could be used on the physical model (see Materials and Methods). A circular incision was made in the silicone to represent cancerous tissue removal during MMS. Water mixed with red food coloring was used to represent blood. It was perfused through the channel left by the monofilament to simulate blood through a small vessel. As the fluid moved to the wound, it began to pool. The ring of the stainless-steel prototype was used to apply circumferential pressure to the wound edges. This caused the vessel to close, representing the achievement of hemostasis. Once pressure was removed, the fluid once again pooled in the wound bed. This process can be seen in Figure 4.

Figure 3. Polished DMLS Printed Prototypes. Stainless-steel devices after supports are removed and devices are polished.

To determine the force required for hemostasis, the experiment was repeated on a scale. The amount of force required to close the vessel using the smaller ring on both devices was recorded for both the cheek and forehead physical models (Table 1). The smaller ring was used because it was most compatible with the incision size. The amount of force ranged from 8N to 15N. These measurements were consistent with the estimate a MMS surgeon gave for how much force he uses on his makeshift hemostatic ring(10-15N). The average pressure required to close the vessel in the cheek model was 8.4N. The average

Table 1. Amount of Force Required to Close the Vessel of the Physical Models Using the Smaller Ring on Each Device.

	Opposite Side (N)	Same Side (N)
30% Thinner Silicone	8.04	9.32
	8.34	8.34
	8.58	7.85
5% Thinner Silicone	12.75	15.2
	12.26	12.75
	12.75	13.73

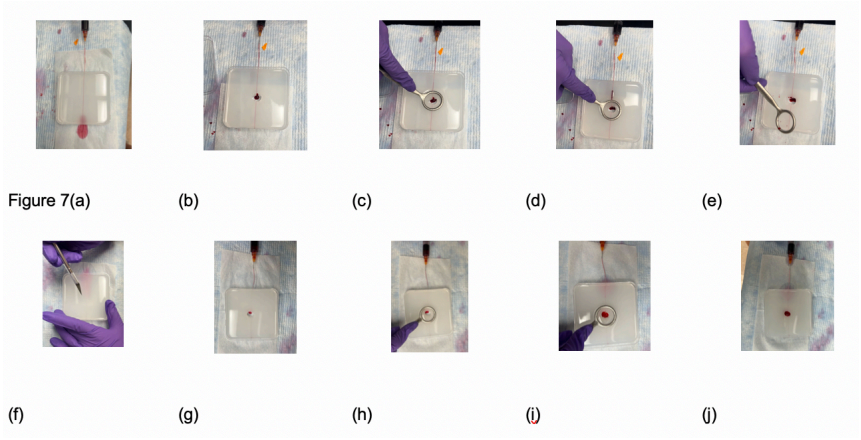

Figure 4. (a-e) **Opposite Side Model used on the 30% Thinner Silicone Model**. (f-j) **Same Side Model used on 5% Thinner Silicone Model.** (a,f) Dyed water to simulate blood perfuses through the model. (b,g) Blood begins entering the cut hole that simulates an incision. (c,h) Stainless steel prototype first applied to surround the incision. (d,i) Prototype able to create hemostasis despite continued flow. (e,f) Prototype removed from model, blood flow returns to normal.

pressure required to close the vessel in the forehead model was 13.2N. Using the design (opposite side or same side) and the tissue (cheek or forehead) as independent variables, a two-way anova test showed that there was no significant difference in the force needed to induce hemostasis ($p = 0.998$).

We created a computational model to test how the cheek and forehead tissues would deform when a load is applied to a stainless-steel ring sitting atop the skin layer (see Materials and Methods). The deformations of the cheek and forehead models can be seen in Table 2. The canal created to represent a blood vessel was expected to close when the load was applied. However, due to limitations in the mesh size available in Autodesk Fusion 360, the vessel never closed. Scaling of the models and of the forces could conceivably overcome this limitation.

Final Steps for Clinical Use

Lastly, the rings of the device needed to be coated in an insulated material so they could be used in tandem with an electrosurgical pen. They were sent to a third party, George Tiemann & Co., to be coated in light blue insulation. Light blue was chosen because it can be discerned from most skin colors and the color of blood.

Discussion

Different clinicians advocated for different designs because of personal preferences in the grip direction of the instrument. Thus, rather than devising a manner to determine a "superior" model, the intention of testing two designs was to prove the efficacy of both prototypes. In showing our polished models (pre-insulation addition) to our clinical advisor, an unexpected advantage of using DLMS over a cast mold, which typically allows for more precise modeling, was discovered. The slight texture left on

Table 2. Tissue Displacement Values in Computational Model with 15N of Pressure Applied to Device

		Ring	Lateral distance from device contact point to tissue (mm)		
			0	10	35
Displacement (mm)	Soft Tissue Simulating Forehead	0.2694	0.2721	0.2032	0.04596
	Soft Tissue Simulating Cheek	1.583	1.564	1.441	0.6388

the surface on our prototypes was noted by one surgeon to be desirable, as it allowed for improved grip.

The computational models showed that our devices would be able to withstand the predicted force application of 10-15 N without any deformation to the device. Despite our secondary computational models being unable to directly show the closing of a 0.3mm vessel due to what we believe to be limitations of the mesh sizing on Autodesk Fusion, the computational model did show that the tissue displaced more greatly directly beneath the contact point of the device than further from the contact point. This means that the device effectively moves the tissue directly below its contact points with minimal disturbance to surrounding tissue. Our physical testing model showed that hemostasis was induced within a reasonable pressure application range. Our clinical advisor noted measured his own typical pressure application range to be between 10 and 15N. Our measured force needed to induce hemostasis on the physical model of 30% thinner and 5% thinner was 8.411N and 13.24N, respectively. These values are within or below the range of force used by the surgeon when using his current version of a hemostatic ring, showing that our prototypes do not require the use of excessive force. The results of the computational models in conjunction with the physical models are encouraging and show the desired success of inducing hemostasis without deformation to the device.

The physical model used to test the stainless-steel printed devices is limited in the fact that only one vessel size was used. In this model, the flow rate prior to application of the device is not of a precise value, as it was controlled manually rather than through the use of a controlled pump. Lastly, the viscosity of the liquid used may be less than in vivo blood as well. While these limitations were present in the physical testing model used, and could be accounted for in future testing model iterations, the model was of quality to allow for the proof of concept of the device.

The computational models used to test the stainless-steel printed devices on soft tissue models are limited in the fact that they do not account for the variation of in vivo tissue values from person to person including the thickness of particular tissue values, or even the precise physical properties of the tissues including Young's Modulus or damping coefficient. It also does not account for pressure application outside of the predicted requirement of pressure needed for device effectiveness. The computational model used to determine if the expected force range of 10-15N would be able to close a 0.3mm vessel also faced limitations. Due to the mesh size of Autodesk Fusion having a lower limit of 0.14mm, it was not able to accurately depict the deformation of our 0.3mm vessel. Thus, despite showing that a 0.3mm vessel could be closed with the precedent force range value in our physical model, we were unable to concretely confirm this with the computational model.

A device that is able to induce hemostasis, requiring only the use of a single hand, will allow clinicians to limit the number of excessive bleeding events in procedures such as MMS. Because the device is also coated in an insulation material, it can be used in conjunction with electrosurgical tools. For usage of electrosurgical tools, such as a cautery pen, to be optimized, there must be minimal fluid present on the surface in which it is used. Thus, inducing hemostasis in turn allows clinicians to optimize usage of electrosurgical devices and further limit excessive bleeding events.

After the completion of this paper, we aim to complete the autoclave testing of the insulation coated prototypes. Moving forward, future work in the continuation of this project may include gaining approval for use of the devices in a clinical trial. Clinical findings may then support gaining greater interest for use of the devices outside of the UVA Hospital and investment in mass production. Future work also may include production of various other models with differing ring or handle sizes to accommodate for both clinician preference and possible other procedures in which the device could be used. Due to turnaround limitations, we were also unable to test the efficacy of the insulation in combination with electrosurgery and electrocautery. In the continuation of this project, this should be tested prior to clinical use.

Materials and Methods

Multiple generations of possible device designs were 3D printed using polylactic acid (Stratasys Dimension printer). Each generation was critiqued and modified to create the subsequent generation of designs. A majority of the early clinical feedback collected and considered for design improvement was from Dr. Mark Russell. After the fourth generation of designs were printed, it was determined that a greater number of clinicians should be consulted for clinical feedback on the designs. All clinicians consulted were employees of the UVA Hospital. To best gauge which features of the device were preferred by clinicians, a questionnaire was developed to gain clinician feedback. Figure 5 shows the five models chosen to be included in the questionnaire given to clinicians at the UVA hospital that perform MMS. The models varied in height (flat, short, normal, tall), handle length (full length, 1cm shorter than full length, and 2cm shorter than full length), ring thickness (thick rings or thin rings), and ring position (rings are oriented on the same plane or rings are oriented on opposite planes). The five models used in the questionnaire were

labeled model A-E. The questionnaire required clinicians to rate particular parameters of the presented models to their liking. These results were then averaged to determine the most optimal models across all clinicians. All clinician feedback was equally weighted in the pursuit of determining a chosen model based on the clinician feedback to ensure the device will be adapted by as many clinicians as possible.

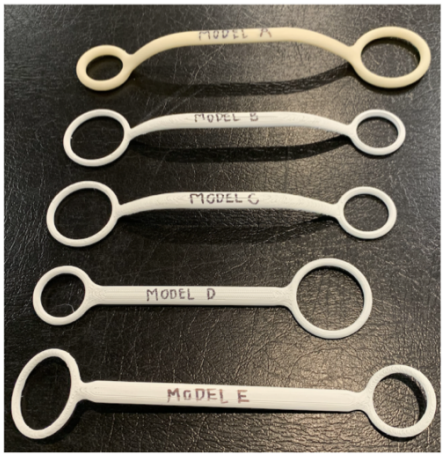

Figure 5. Models Included in Hemostatic Ring Questionnaire Presented to Clinicians.

Prior to finalizing design choice, computational models were made and simulations were performed to test the performance of various models. Each of the five models used in the questionnaire underwent a simulation in which 15N of force was applied to the device handle while one of the rings was fixed (the ring was fixed to simulate its inability to move when applied to the skin). The safety factor of each model was recorded upon the completion of the simulation. These values, in conjunction with the results of the questionnaire (Supplementary Figure 2) were used to determine the optimal model for stainless steel production. Two models, Model B and Model E, resulted in having similar preference and strength values. Because the two models were so distinct from each other, it was decided to produce both designs in stainless steel.

A secondary computational simulation was then conducted to test the failure load of each of the chosen models. The failure load values show the pressure required to severely damage the integrity of the device. Our clinical advisor estimated that he uses a maximum force of 15N to induce hemostasis using the ring handle of a hemostat. The failure loads were found to be 70.0N and 87.0N for the "Ring Opposite Side Prototype" and the "Ring Same Side Prototype", respectively. These values are significantly higher than this threshold. This shows that it is not expected that either design choice would be deformed or break when used for the intended clinical application.

A third simulation was conducted to test the effect of the stainless-steel ring pressure on soft tissue. Models including skin, fat, and muscle layers of the forehead and the cheek were created. Values were found through literature to determine the physical properties of skin, fat and muscle (Supplementary Figure 3). A hole simulating an incision from MMS was cut into the skin layer. A 0.3mm hole running parallel to the skin was also cut into the skin layer to simulate a blood vessel. The aim of this simulation was to determine if the constructed vessel would close under the pressure of the ring application with the force expected to be used in the clinical setting (10-15 N). However, when the simulation was run with these force values, despite seeing a large displacement in the tissue directly under the contact points of the ring devices, the simulated vessel did not close. The simulation was then run with an extreme force value of 100N. The vessel still did not close. This leads us to believe that the failure of closure was due to the mesh size of the simulation in comparison to the vessel size. To alternatively achieve proof of concept for the 0.3mm vessel size, the displacement of the ring was compared to the displacement of the tissue directly beneath, 10mm away, and 35mm away from the contact point as seen in Table 2. We would expect to see the tissue directly under the contact point to have the same displacement as the ring itself, and tissue further away to have less displacement. This shows that pressure application through the ring is able to compress the tissue beneath it.

A physical model was also made using silicone; 30% thinner was used to simulate the cheek, and 5% thinner was used to simulate the forehead. Two 0.5mm holes were drilled into opposite walls of the petri dish halfway between the bottom and top. 0.3mm diameter monofilament was strung through both holes until it was taught. PE 50 tubing was inserted 1cm into one side of the petri dish with the monofilament running through it. The loose ends of the monofilament were taped down. Two mixtures of Smooth-On silicone were made to replicate the cheek and forehead tissues. The cheek model used 30% thinner and the forehead model used 5% thinner to represent the various stiffnesses. The mixtures were poured into their respective petri dishes so that the monofilament was covered by at least a centimeter of silicone. The models were allowed to set in a vacuum for approximately six hours. Once the models were set, the monofilament was removed to reveal a canal that would be used to replicate a blood vessel. A syringe could then be attached to the PE 50 tubing to allow for liquid perfusion. Red-dyed liquid was then allowed to flow through the canal in the silicone simulating blood flow. An incision was then cut, and the device was used to induce

hemostasis. The setup of this physical model can be seen in Figure 6.

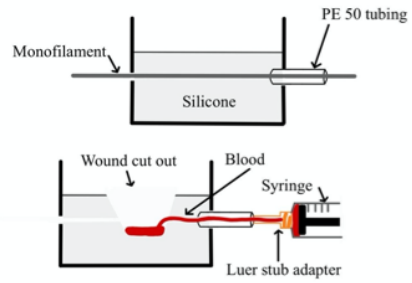

Figure 6. Spliced Side View of Physical Model Created for Prototype Testing

End Matter

Author Contributions and Notes

P.K.O and R.C.B designed research, P.K.O and R.C.B performed research, P.K.O and R.C.B analyzed data; and P.K.O and R.C.B wrote the paper.
The authors declare no conflict of interest.

Acknowledgments

The authors thank Dr. William Guilford for his guidance and support. The authors thank Dr. Mark Russell for proposing the project and for his clinical expertise. The authors thank the NIH for funding the UVA BME Clinical Scholars Program where the project was born.

References

(1) Mohs Surgery. *The Skin Cancer Foundation*.
(2) Skin cancer https://www.aad.org/media/stats-skin-cancer (accessed 2021 -09 -22).
(3) Lee, J.; Russell, M. A. Ring Hemostasis: Preserving the View. *J. Am. Acad. Dermatol.* **2021**. https://doi.org/10.1016/j.jaad.2021.08.032.
(4) Bunick, C. G.; Aasi, S. Z. Hemorrhagic Complications in Dermatologic Surgery. *Dermatol. Ther.* **2011**, *24* (6), 537–550. https://doi.org/10.1111/j.1529-8019.2012.01454.x.
(5) Walsh, E. Pressure Ring for Hemostasis. *AMA Arch. Dermatol. Syphilol.* **1950**, *62* (5), 718–719.
(6) Osbourn, R. A. Plastic Pressure Ring for Hemostasis. *AMA Arch. Dermatol. Syphilol.* **1954**, *69* (5), 612–613.
(7) Pawlaczyk, M.; Lelonkiewicz, M.; Wieczorowski, M. Age-Dependent Biomechanical Properties of the Skin. *Adv. Dermatol. Allergol. Dermatol. Alergol.* **2013**, *30* (5), 302–306. https://doi.org/10.5114/pdia.2013.38359.
(8) Li, C.; Guan, G.; Reif, R.; Huang, Z.; Wang, R. K. Determining Elastic Properties of Skin by Measuring Surface Waves from an Impulse Mechanical Stimulus Using Phase-Sensitive Optical Coherence Tomography. *J. R. Soc. Interface* **2012**, *9* (70), 831–841. https://doi.org/10.1098/rsif.2011.0583.
(9) Skin mechanical properties and modeling: A review - Hamed Joodaki, Matthew B Panzer, 2018 https://journals-sagepub-com.proxy01.its.virginia.edu/doi/10.1177/0954411918759801 (accessed 2022 -03 -27).
(10) Liang, X.; Boppart, S. A. Biomechanical Properties of In Vivo Human Skin From Dynamic Optical Coherence Elastography. *IEEE Trans. Biomed. Eng.* **2010**, *57* (4), 953–959. https://doi.org/10.1109/TBME.2009.2033464.
(11) Boyer, G.; Laquièze, L.; Le Bot, A.; Laquièze, S.; Zahouani, H. Dynamic Indentation on Human Skin in Vivo: Ageing Effects. *Skin Res. Technol.* **2009**, *15* (1), 55–67. https://doi.org/10.1111/j.1600-0846.2008.00324.x.
(12) Tensile strength - Soft-Matter http://soft-matter.seas.harvard.edu/index.php/Tensile_strength (accessed 2022 -03 -27).
(13) Dynamic Tensile Properties of Human Skin. **2012**, 9.
(14) Jacquemoud, C.; Bruyere-Garnier, K.; Coret, M. Methodology to Determine Failure Characteristics of Planar Soft Tissues Using a Dynamic Tensile Test. *J. Biomech.* **2007**, *40* (2), 468–475. https://doi.org/10.1016/j.jbiomech.2005.12.010.
(15) A Method for Characterization of Tissue Elastic Properties Combining Ultrasonic Computed Tomography With Elastography - Glozman - 2010 - Journal of Ultrasound in Medicine - Wiley Online Library https://onlinelibrary-wiley-com.proxy01.its.virginia.edu/doi/10.7863/jum.2010.29.3.387 (accessed 2022 -03 -27).
(16) Then, C.; Menger, J.; Benderoth, G.; Alizadeh, M.; Vogl, T. J.; Hübner, F.; Silber, G. A Method for a Mechanical Characterisation of Human Gluteal Tissue. *Technol. Health Care Off. J. Eur. Soc. Eng. Med.* **2007**, *15* (6), 385–398.
(17) Adipose tissue volume measured by magnetic resonance imaging and computerized tomography in rats | Journal of Applied Physiology https://journals-

physiology-org.proxy01.its.virginia.edu/doi/abs/10.1152/jappl.1991.70.5.2164 (accessed 2022 -03 -27).

(18) Tissue and force modelling on multi-layered needle puncture for percutaneous surgery training | IEEE Conference Publication | IEEE Xplore https://ieeexplore.ieee.org/document/7844684 (accessed 2022 -04 -05).

(19) Lackey, D. E.; Burk, D. H.; Ali, M. R.; Mostaedi, R.; Smith, W. H.; Park, J.; Scherer, P. E.; Seay, S. A.; McCoin, C. S.; Bonaldo, P.; Adams, S. H. Contributions of Adipose Tissue Architectural and Tensile Properties toward Defining Healthy and Unhealthy Obesity. *Am. J. Physiol. - Endocrinol. Metab.* **2014**, *306* (3), E233–E246. https://doi.org/10.1152/ajpendo.00476.2013.

(20) Elastic modulus of skeletal muscle - Mammals - BNID 106647 https://bionumbers.hms.harvard.edu/bionumber.aspx?s=n&v=3&id=106647 (accessed 2022 -03 -28).

(21) Wheatley, B. B.; Morrow, D. A.; Odegard, G. M.; Kaufman, K. R.; Donahue, T. L. H. Skeletal Muscle Tensile Strain Dependence: Hyperviscoelastic Nonlinearity. *J. Mech. Behav. Biomed. Mater.* **2016**, *53*, 445–454. https://doi.org/10.1016/j.jmbbm.2015.08.041.

(22) Siracusa, J.; Charlot, K.; Malgoyre, A.; Conort, S.; Tardo-Dino, P.-E.; Bourrilhon, C.; Garcia-Vicencio, S. Resting Muscle Shear Modulus Measured With Ultrasound Shear-Wave Elastography as an Alternative Tool to Assess Muscle Fatigue in Humans. *Front. Physiol.* **2019**, *10*.

(23) FAT vs. MUSCLE. *Banister Nutrition, LLC | OKC Dietitian | Nutrition Specialists*, 2014.

(24) Mohamed, A.; Alkhaledi, K.; Cochran, D. Estimation of Mechanical Properties of Soft Tissue Subjected to Dynamic Impact. *J. Eng. Res.* **2014**, *2* (4), 26. https://doi.org/10.7603/s40632-014-0026-8.

(25) Kuthe, C. D.; Uddanwadiker, R. V.; Ramteke, A. Experimental Evaluation of Fiber Orientation Based Material Properties of Skeletal Muscle in Tension. *Mol. Cell. Biomech. MCB* **2014**, *11* (2), 113–128.

Supplementary Figure 1. Prior Attempts at a Pressure Ring for Hemostasis. A) Walsh, 1950 and B) Osbourn, 1954

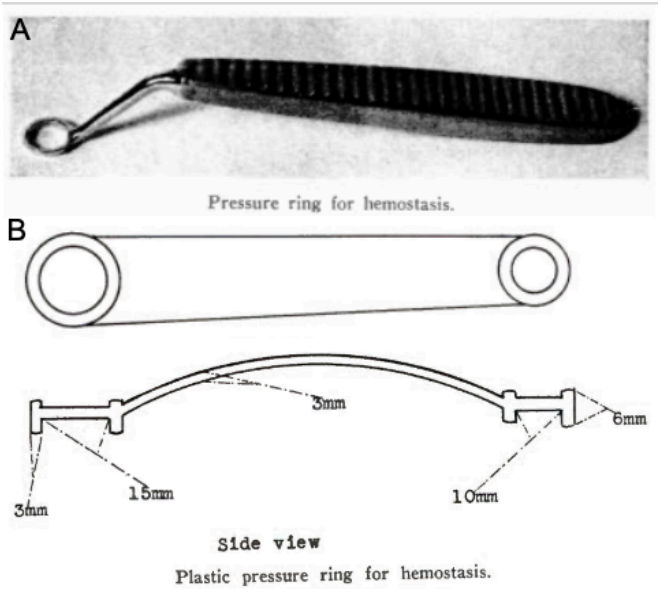

Supplementary Figure 2. Hemostatic Ring Questionnaire Results.

	Mark Russell, MD	Darren Guffey, MD	Henry Zu, MD
Estimated Necessity	Minor improvement to what is currently used	Nothing else can solve this problem	Nothing else can solve this problem
Estimated Use	2-3 times/week	2-3 times/week	2-3 times/week
Preferred Ring Thickness	Thin	Thin	Thin
Preferred Handle Height	Flat	High	Flat
Preferred Handle Length	Short	Short	Medium
Overall Ranking (best first)	D C B E A	E B C A D	E G3[1] C B A

Supplementary Figure 3. Values Required for Virtual Simulation Testing

	Young's Modulus		Poisson Ratio		Shear Modulus (kPa)		Density (g/ml)		Damping Coefficient (N s/m)		Yield Strength (MPa)*		Tensile Strength (MPa)	
	Cheek	Forehead	Cheek	Forehead	Cheek	Forehead	Cheek	Forehead	Cheek	Forehead	Cheek	Forehead	Cheek	Forehead
Skin	**50-2000 kPa[7]**	**50-2000 kPa[7]**	0.48[8]	0.48[8]	49.8[9]	49.8[9]	1.02[10]	1.02[10]	0.062-0.074[11]	0.062-0.074[11]	15[12]	15[12]	27.2[13]	4.6 , 27.2[14]
Fat	**34 kPa[8]**	**34 kPa[8]**	0.5[15]	0.5[15]	1.182[16]	1.182[16]	0.9[17]	0.9[17]	1[18]	1[18]	0.013 28[19]	0.132 8[19]	0.013 28[19]	0.013 28[19]
Muscle	**10 kPa[20]**	**10 kPa[20]**	0.47[21]	0.47[21]	10[22]	10[22]	1.1[23]	1.1[23]	2[24]	2[24]	0.44[25]	0.44[25]	0.44[25]	0.44[25]

*Yield strength matches the tensile strength as we expect the specimen to remain in the elastic region. Yield strength values for skin were found directly.